

## Polymer and Soft Matter Research at Diamond Light Source

N. J. Terrill, A. Bombardi, F. Carlà, G. Cinque, M. J. Derry, A. Milsom, G. Siligardi, T. Snow, P. D. Topham, X. B. Zeng & T. Zinn

To cite this article: N. J. Terrill, A. Bombardi, F. Carlà, G. Cinque, M. J. Derry, A. Milsom, G. Siligardi, T. Snow, P. D. Topham, X. B. Zeng & T. Zinn (2023): Polymer and Soft Matter Research at Diamond Light Source, Synchrotron Radiation News, DOI: [10.1080/08940886.2023.2207456](https://doi.org/10.1080/08940886.2023.2207456)

To link to this article: <https://doi.org/10.1080/08940886.2023.2207456>



© 2023 The Author(s). Published with license by Taylor & Francis Group, LLC



Published online: 02 Jun 2023.



Submit your article to this journal [↗](#)



Article views: 22



View related articles [↗](#)



View Crossmark data [↗](#)

# Polymer and Soft Matter Research at Diamond Light Source

N. J. TERRILL,<sup>1</sup> A. BOMBARDI,<sup>1</sup> F. CARLÀ,<sup>1</sup> G. CINQUE,<sup>1</sup> M. J. DERRY,<sup>2</sup> A. MILSON,<sup>3</sup> G. SILIGARDI,<sup>1</sup> T. SNOW,<sup>1</sup> P. D. TOPHAM,<sup>2</sup> X. B. ZENG,<sup>4</sup> AND T. ZINN<sup>1</sup>

<sup>1</sup>Diamond Light Source, Diamond House, Harwell Science and Innovation Campus, Didcot, UK

<sup>2</sup>Aston Advanced Materials Research Centre, Aston University, Birmingham, UK

<sup>3</sup>Geography, Earth and Environmental Sciences, University of Birmingham, Birmingham, UK

<sup>4</sup>Department of Materials Science and Engineering, Sheffield University, Sheffield, UK

## Introduction

Polymer and soft matter research have played an integral part in the development of Diamond Light Source ever since the facility took its first users in 2007. Early experiments explored highly swollen cubic lipid scaffolds [1] using pressure [2] to elicit phase transitions and liquid-crystal engineering [3]. The facility now comprises 33 active synchrotron instruments, together with 13 electron microscopes, and other offline facilities. Diamond has an active polymer and soft matter science program exploring new phase space as well as many *in operando* studies. Later in the article, we will describe the opportunities available to this research community from the planned machine upgrade, which includes a higher-energy, lower divergence ring with better coherence [4].

## Polymer and soft matter science at Diamond

It is often overlooked that the simplest measurements can offer glimpses into the intricate morphologies of materials, including block copolymers, colloids, and liquid crystals. The phase of a material often dictates its physical properties. Gregory et al. utilized small-angle X-ray scattering (SAXS) to identify phases of a series of well-defined triblock polyester thermoplastic elastomers [5] to confirm why their materials have the rheological properties they do. With this knowledge, they made simple modifications to bio-derived degradable polyesters and polycarbonates to deliver superior performances, using SAXS to monitor phase behavior. This was achieved by appending metal-carboxylate functionalities to the polymer chains without compromising the desirable morphology (hexagonally packed cylinders) for elastomeric properties [6, 7]. They also used measurements provided by the laboratory source managed by Diamond/I22 (DL-SAXS) [8] to help understand the nuances in solid-state battery development that might help deliver greater retention. Polyether and CO<sub>2</sub>-derived polycarbonate blocks loosely arranged into a particular nanoscale morphology exposed higher lithium-ion conductivities by providing channels for ions to percolate. Coupled with elasticity, the polymers act as conducting binders buffering detrimental volume changes in composite cathodes (Figure 1). This small element made a marked difference to the cycling performance of solid-state batteries, which are widely earmarked as game changers for electric vehicles. Rapid access to DL-SAXS offers the advantage of screening numerous

block copolymer compositions, molar masses, and chemistries in one go to identify lead samples for application testing.

The work of Zeng et al. on I22 as well as I07, I16, and XMAS at the ESRF, combining transmission small- and wide-angle X-ray diffraction (SAXD/WAXD) from powder samples with grazing incidence XRD from surface-oriented samples, has revealed many complex self-assembled structures of liquid crystal (LC)-based materials. These include supra-molecules from dendrons, honeycombs, bicontinuous cubic and other complex phases from T- and X-shaped molecules, LC covered nanoparticles, and columnar liquid crystals confined in nanopores [9–19]. One example explored the spontaneous formation of long-range ordered helical columns, from achiral molecules with either straight or bent-rod cores without the addition of chiral molecules (Figure 2). The helicity of the column originates from twisting of molecule directions between neighboring molecular strata, a compromise which maintains a high degree of  $\pi$ - $\pi$  stacking between the rigid cores of the molecules while avoiding flexible end-tail clashes. They form on a complex lattice (*Fddd*) comprising eight columns per unit cell, four of each hand, giving an antiferrochiral structure. As the molecular cores' stacking improves, the fluorescent group's bandgap is lowered, giving them exciting light emitting properties [9].

The group also carried out the first resonant diffraction experiment on unusual magnetically oriented twist-bend nematic phases at the

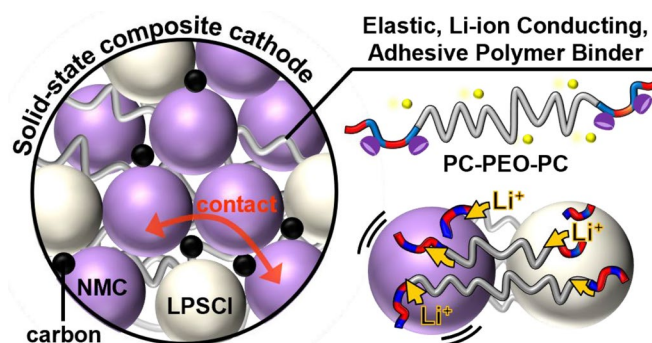


Figure 1: Schematic of triblock polymers investigated by SAXS, comprising polycarbonate (PC) and polyethylene oxide (PEO) for improved next-generation solid-state battery performance (redrawn from [8] Open Access CC-BY: <https://creativecommons.org/licenses/by/4.0/>).

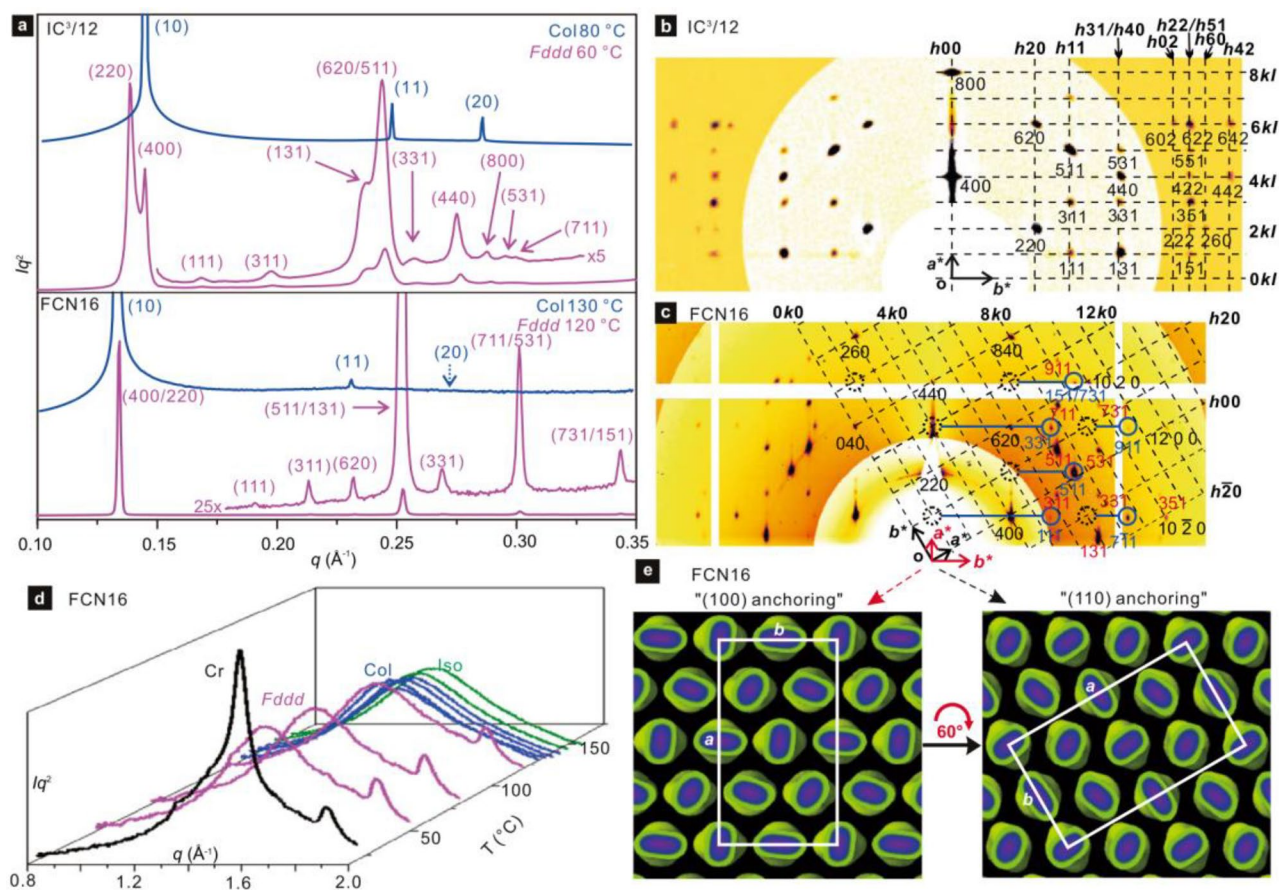


Figure 2: X-ray diffraction results. (a) Transmission powder SAXS curves of Col and Fddd phases of a bent-core (IC3/12) and a straight-core compound (FCN16). The dominance of (220) and (400) diffraction peaks shows that in both compounds the columns pack on a nearly hexagonal lattice. (b, c) GISAXS patterns of Fddd phase of IC3/12 and FCN16. The background was subtracted and the higher- $q$  zone was intensity-enhanced. The partial reciprocal  $hk0$  lattice plane is superimposed, with some  $hkl$  spots in (c) circled blue and connected to their  $hk0$  base by blue row lines. Reflections in (c) come from two orientations with (110) and (100) planes anchored on the Si substrate; reflections in red are from the latter. (d) Evolution of powder WAXS of FCN16 on heating; note the  $3.5 \text{ \AA}$  peak ( $q = 1.8 \text{ \AA}^{-1}$ ) in the Fddd and crystal phases. (e) Real space FCN16: in both orientations, the LC faces substrate with a dense plane of columns (unit cell in white) (redrawn from [9] Open Access CC-BY: <https://creativecommons.org/licenses/by/4.0/>).

selenium edge on I22. The resonant diffraction spots (Figure 3) provided direct experimental evidence that the molecular director forms a helix with a 9–12 nm pitch in the  $N_{ib}$  phase. Observation of long-range orientational order without positional order is made possible using the ability to precisely tune the X-ray energy at I22, the orientation of the sample using magnetic field, combined with good temperature control. Unprecedentedly high helix orientation was observed and enabled deconvolution of global and local order parameters. Combined with simultaneously recorded resonant and non-resonant SAXS and wide-angle X-ray scattering (WAXS) data, the results allowed construction of a locally layered molecular model of the  $N_{ib}$  phase, where the average twisted conformation of each molecule was idealized as a helical segment, matching the local heliconical director field [20].

Following real-time morphological changes [21] and chemical reactions has always been a feature of polymer studies at synchrotron radiation (SR) sources [22]. Topham and co-workers have integrated complex sam-

ple environments [21, 23] to study reversible addition–fragmentation chain transfer (RAFT) polymerization [24], an important way of controlling the morphology of well-defined amphiphilic diblock copolymers from a wide range of functional monomers, including terpene-derived renewable monomers [25, 26]. RAFT polymerization has been utilized to generate a host of block copolymer nanoparticles using an emerging synthetic tool termed polymerization-induced self-assembly (PISA). Derry et al. first used in-situ SAXS measurements to extract important mechanistic information on the formation and growth of diblock copolymer nanoparticles (spherical micelles, worm-like micelles and vesicles) during RAFT-mediated dispersion PISA in mineral oil [27]. An in-situ temperature-controlled, stirrable reaction cell was designed and developed to demonstrate RAFT-mediated emulsion PISA (Figure 4). The versatility and importance of in-situ SAXS measurements in monitoring dynamic nanoparticle evolution was most recently showcased by Fielden et al. The researchers followed an isotropic-to-anisotropic nanoparticle evolution

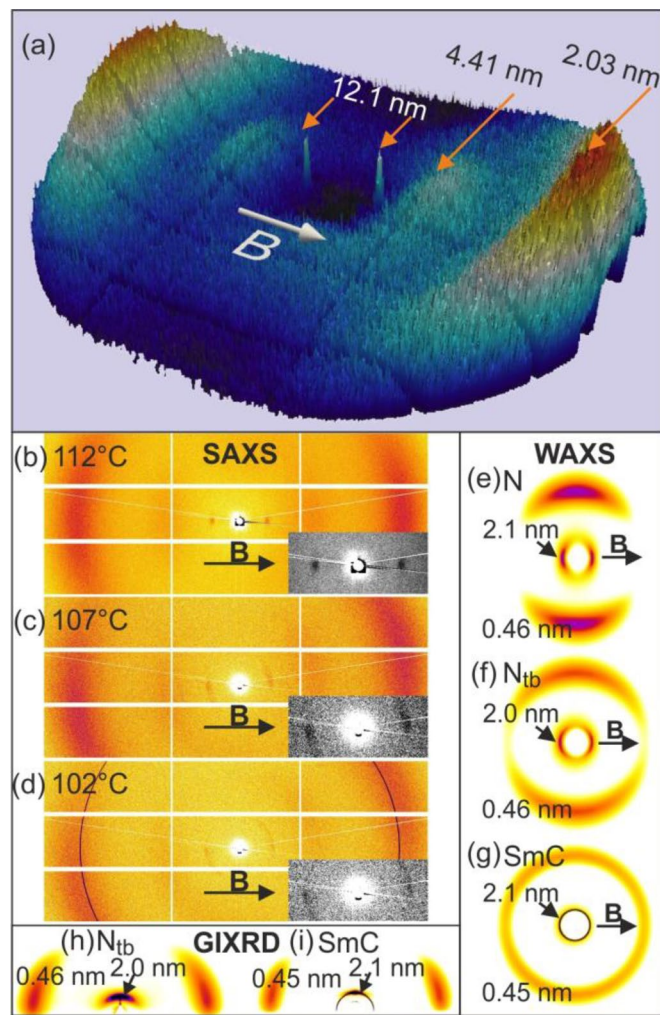


Figure 3: (a) Surface plot of the SAXS diffractogram of the  $N_{tb}$  phase at 112°C aligned in magnetic field,  $E_i = 12.658$  keV. (b)(c)(d) 2D SAXS patterns of the  $N_{tb}$  phase at 112°C, 107°C, and 102°C, with zoom-in of the sharp resonant SAXS peaks. (e–g) Transmission WAXS patterns of the compound in the (e) N, (f)  $N_{tb}$ , and (g) SmC phase. (h–i) Wide-angle GIXRD patterns of the compound in the (h)  $N_{tb}$  and (i) SmC phase; smectic layers are parallel to the horizontal substrate (redrawn from ref. [20] Open Access CC-BY: <https://creativecommons.org/licenses/by/4.0/>).

on I22 via rapid fusion and rearrangement events involving block copolymer particles initially synthesized via ring-opening metathesis polymerization (ROMP) [28].

One advantage synchrotrons have over lab facilities are the smaller beamsizes that can be obtained, while still providing excellent flux. At Diamond, I22 routinely offers 10 micron beams for studying soft matter. Milsom et al. have utilized this to study organic aerosols found in air pollution [29]. The group installed an acoustic levitator to hold individual aerosol droplets in the beam for study. They found that molecular self-organization significantly increased the chemical lifetime of common surfactant fatty acid cooking emissions. The small beam

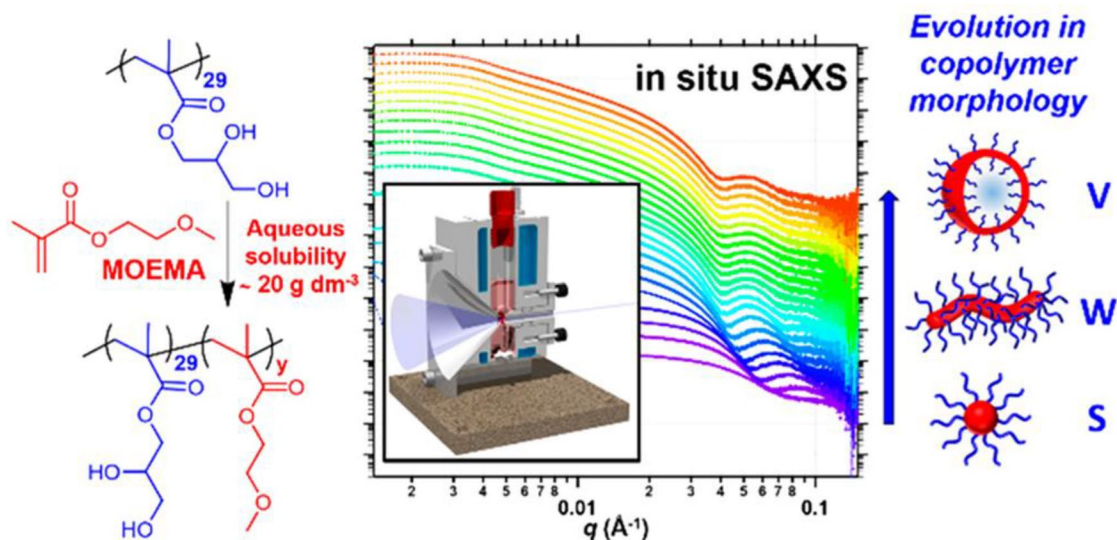
helped identify a product crust that formed around the levitated droplets during simulated atmospheric ageing, thought to inhibit particle reactivity and increase the chemical lifetime of atmospheric aerosol components. Milsom et al. also took advantage of the small beam to measure reaction kinetics in this self-organized fatty acid system [30]. Data gathered from these experiments informed detailed models of atmospheric aerosol kinetics and showed that fatty acids could last for days in the atmosphere when they form these viscous self-organized phases, potentially impacting our health and larger areas of the atmosphere and environment than would have been expected [31].

While SAXS provides bulk information, the use of grazing incidence techniques including grazing incidence small-angle X-ray scattering (GISAXS), grazing incidence X-ray diffraction (GIXD), surface X-ray diffraction (SXRD) in combination with X-ray reflectivity (XRR) allow the investigation of self-assembly processes and the structural effects of chemical reactions at interfaces and in 2D systems. The same length scales explored by SAXS can be accessed with GISAXS, providing information on the organization of polymer films and molecular crystals [17–19] confined on surfaces. The degree of anisotropy at a surface/interface acting as an anchoring point for the molecules forming the film can be responsible for a possible difference between the physicochemical properties of films and bulk systems.

Model 2D systems allow creation of simplified case studies for biochemical and physicochemical problems. Phospholipids are used to model mammalian cellular membranes [32, 33] by creating layers and bilayers on solid and liquid substrates. The use of XRR (a technique that works independently from the structural order) for investigating layering at the interface by measuring film thickness, roughness, and density distribution along the direction perpendicular to the surface complements the information gathered using scattering/diffraction techniques. Information regarding molecular packing density, tilt angles, and the presence of water molecules influencing the hydrogen bonding networks around the polar heads can be measured as a function of the chemical environment and in response to external stimuli (applied electric field, illumination).

X-ray scattering and XRR experiments from liquid/air and liquid/liquid interfaces have been performed on I07 with a double crystal deflector [34] that allows a variable angle of incidence of the beam on a liquid surface. A general-purpose Langmuir trough setup, largely used for characterization of bio-mimetic cellular membrane systems, with a particular focus on lipid packing and solvation, has been developed at I07 along with other specialized setups for liquid interfaces. The possibility of changing the layer compression and perturbing the system with external stimuli (e.g., addition of a foreign molecule to the layer) allows one to draw a relation between orientational and conformational changes at the molecular level and phase transitions in films [33, 35].

Although reflectivity and scattering are the most obvious techniques for the characterization of organic molecule-based thin films, Brugman et al. [36] used surface crystallography (SXRD) to investigate the adhesion of carboxylic acid molecules on mineral surfaces. The authors used calcite (104) and mica (001) as model systems for investigating the



Q3 Figure 4: In-situ RAFT polymerization using the custom-built cell (redrawn from [23] Open Access CC-BY: <https://creativecommons.org/licenses/by/4.0/>). S= spheres, W = wormlike, V = vesicles.

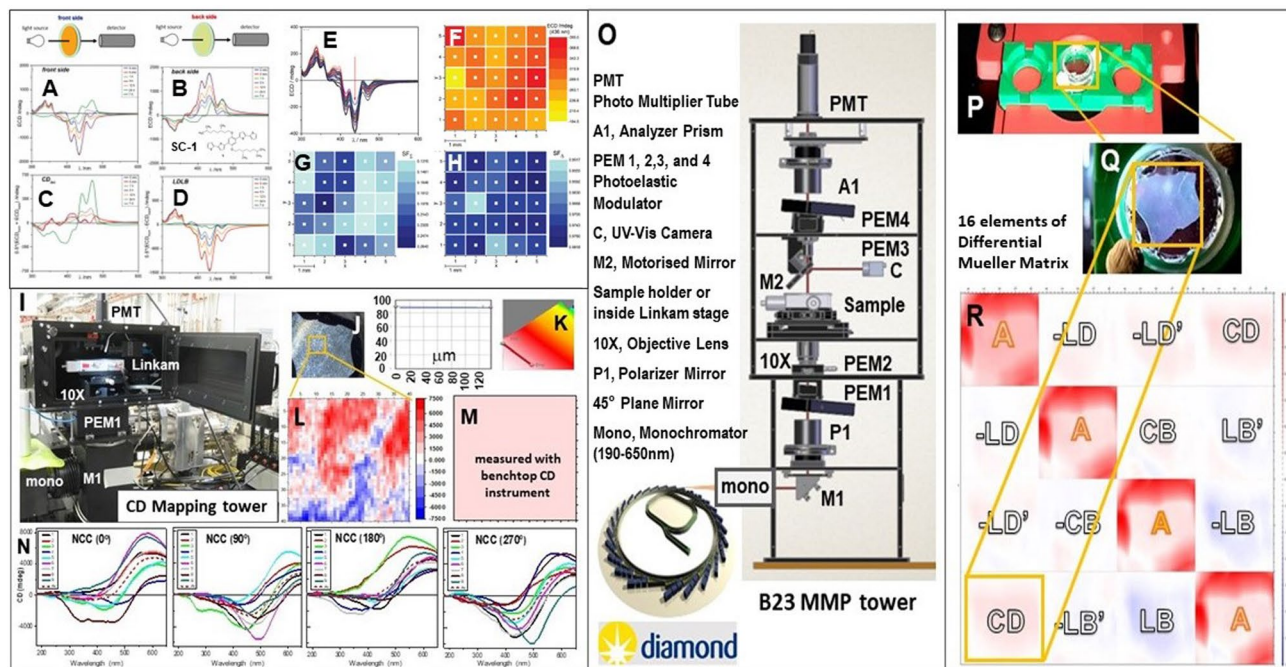


Figure 5: Examples of the capability on B23. For more detail on each, please see Figure 2 from [37] Open Access CC-BY: <https://creativecommons.org/licenses/by/4.0/>.

adsorption behavior at the base of the differences of the oil–solid interactions in carbonate and sandstone reservoirs.

While X-rays form the majority of polymer and soft matter activities at Diamond, it is important to note that other wavelengths play as essential a role. Circular dichroism using UV wavelengths on B23 has been employed to characterize conformational and supramolecular structure of chiral entities from molecules such as

drugs,  $\pi$ -conjugated systems with optoelectronic properties, j-aggregates for plasmonic, liquid crystals forming twisted nematic phases, to polymers such as proteins, nucleic acids (DNA and RNA), carbohydrates, and nanocrystalline cellulose. Since 2020, the Mueller matrix polarimetry tower (MMP) [37], operating between 190 and 650 nm, has been primarily devoted to the study of solid-state films and hydrogels (Figure 5).

In solution the media is isotropic, but in the solid-state linear anisotropies such as linear dichroism (LD) and linear birefringence (LB) can be significant and dominate the chiral anisotropy: circular dichroism (CD) and its counterpart circular birefringence (CB). LD and LB can distort the measured CD spectral features when measured with CD spectropolarimeters. Using the MMP, the anisotropies can be decomposed for non-depolarizing materials and interpret their chiroptical properties to confirm that the material is chiral or that chiral domains are present. The MMP tower is used to study the optical LD, LB, and chiroptical properties CD and CB of thin films of chiral materials such as polymers, biopolymers, optoelectronics, hydrogels, J-aggregate systems, and twisted nematic liquid crystals. B23's MMP is unique for mapping thin chiral materials at the highest spatial resolution, 50 microns, and as a function of temperature ( $-170^{\circ}\text{C}$  to  $+300^{\circ}\text{C}$ ) and static 1.3 T magnetic field, parallel or perpendicular to the propagation of the incident beam. Organic semiconductors based on chiral  $\pi$ -conjugated polymers and oligomers constituting innovative optoelectronic devices necessitate the ability to control and monitor the supramolecular architecture of these materials. Articles by Albano et al. [38], Clowes et al. [39], and Killalea et al. [40] illustrate the continuous development in electronic CD imaging (ECDi or simply CDi) enabling users to explore the chiroptical properties of thin films more efficiently. Mapping at this spatial resolution using B23-ECDi revealed several species to coexist in the mesoscopic chiral domains, likely due to different aggregated phases, which could not be detected with benchtop ECD instruments. These studies showed how CD, unlike optical microscopy, can see the handedness of the supramolecular structure.

Infra-red wavelengths are key in studying soft matter at the molecular level. Crude estimations suggest that  $\sim 23\%$  of the world's total energy consumption is from tribological contacts; e.g., in lubricants. Predictions that the friction coefficient should vanish for certain configurations of contacting crystalline surfaces, named "superlubricity," have been made and proposed at a  $\mu < 0.01$  threshold [41]. Previous studies of 1-dodecanol EHL friction suggested that a very low value could be achieved, but the

physicochemical changes leading to low friction in n-alcohols remain scientifically unclear. Using a tribometer, diamond anvil cell (DAC), and synchrotron-based IR microspectroscopy, plus differential scanning calorimetry (DSC) experiments (Figure 6), scientists at B22 showed that liquid 1-dodecanol undergoes a pressure-induced solidification when entrained into EHL contacts [42]. At moderate temperatures and pressures, 1-dodecanol forms a polymorph that exhibits robust macroscale superlubricity, which is facilitated by the formation of lamellar, hydrogen-bonded structures of hexagonally close-packed molecules, which promote interlayer sliding. This novel superlubricity mechanism is similar to that proposed for the two-dimensional materials commonly employed as solid lubricants, but it also enables the practical advantages of liquid lubricants to be maintained. This is the first demonstration of macroscale superlubricity in an EHL contact, lubricated by a nonaqueous liquid that arises from bulk effects rather than tribochemical transformations at the surfaces. Since the superlubricity observed results from phase transformations, it is continuously self-replenishing and is insensitive to surface chemistry and topology, with potential improvements in efficiency and durability for mechanical applications.

Liquid-liquid transitions (LLT) between two amorphous phases in a single-component are still scientifically controversial. Known examples observed in the supercooled state suggest a connection with vitrification and crystallization inhibition. Scientists at B22 have investigated triphenyl phosphite (TPP) as an exemplary molecular liquid, and showed that its transition is caused by competition between liquid structures that mirror two crystal polymorphs [43]. Time-resolved synchrotron-based FTIR microspectroscopy (on minute to hour timescales) was performed to follow structural changes during a quench, leading to a LLT or crystallization using a cryostat device cooling by  $\text{LN}_2$  flow (Figure 7). The IR spectrum is a proxy for the local molecular packing in the liquid or crystal: four canonical spectra were identified in Figure 7a. IR imaging experiments in Figure 7b showed spatially that the molecular changes are confined to the growing droplets of liquid 2, rather than gradually over the entire sample.

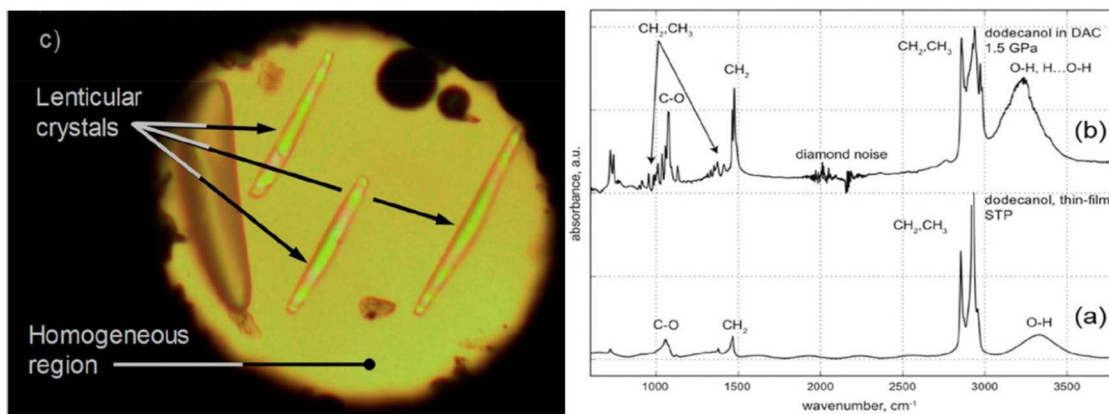


Figure 6: Polarized-light images of a DAC chamber with 1-dodecanol at  $25^{\circ}\text{C}$  (a) and  $\sim 0.15$  GPa (c). The field of view is  $400\mu\text{m}$ . FTIR spectra from a DAC at  $25^{\circ}\text{C}$  and  $0.1$  MPa (a) and  $1.5$  GPa (b) (redrawn from [42]). Reprinted (adapted) with permission from T. Reddyhoff et al., ACS Appl. Mater. Interfaces. 13 (7), 9239 (2021). doi:10.1021/acsami.0c21918. © 2021 American Chemical Society.

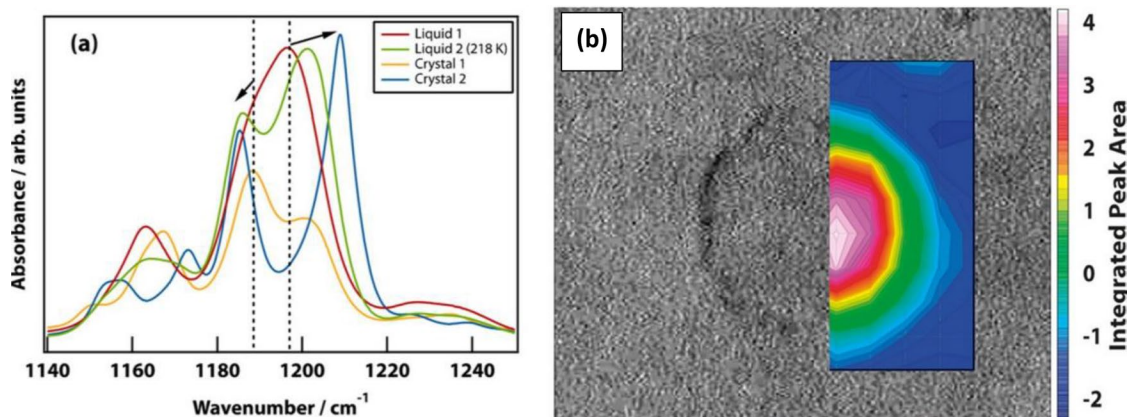


Figure 7: (a) Infrared spectra of liquid 1, liquid 2, crystal 1, and crystal 2 in the 1140–1250  $\text{cm}^{-1}$  range. (b) Infrared image overlaying a bright field image of a droplet of liquid 2 produced at a quench temperature of 224 K. Color scale corresponds to main peak 1200–1215  $\text{cm}^{-1}$  intensity (liquid 2) (redrawn from [43] Open Access CC-BY: <https://creativecommons.org/licenses/by/4.0/>).

These new insights, based on firm experimental results, may underpin a new phase of research into the physical-chemistry basis of LLTs in molecular liquids, their occurrence, and generally into supercooling and vitrification, with the interplay of geometric and kinetic frustration; e.g., even toward better understanding of LLT in water and its polymorphs.

## Beamlines carrying out polymer or soft matter research at Diamond

B22, a Multimode InfraRed Imaging and Microspectroscopy (MIRIAM) beamline [44] in operation since 2009, has led the development and research in several synchrotron-based IR methods. In full-field IR imaging by focal plane array (FPA) detector, the highest magnification in life sciences allows real-time biomolecular monitoring within living mammalian cells [45], now using adaptive optics [46]. With scanning IR microscopy, the highest spectral quality is gained by a diffraction-limited resolution; e.g., physical behavior of metal-organic frameworks [47] and/or in-situ/operando chemistry. This is complemented by Tera-Hertz (THz) capabilities via Fourier Transform IR (FTIR), allowing exploration of the sub-eV energy range of soft condensed matter [48]. Recently, a new, unique, nanospectroscopy end station has been added, coupling an atomic force microscope with the synchrotron IR microprobe. Both scattering nearfield optical microscopy (SNOM) and photothermal modes are possible, achieving molecular sensitivity and resolution in the 10 to 100 nm [49].

B23, a highly collimated microbeam generated for synchrotron radiation circular dichroism (SRCD) [50] and, since 2020, also for Mueller matrix polarimetry (MMP) [37], is unique in the world. B23 operates two end-stations: modules A and B to accommodate a variety of sample environments and experiment types. Module A operates in the 170–550 nm region and selecting the appropriate sample chamber.

I07, a surface and interface diffraction beamline [51] in operation since 2010, works in the energy range between 6 and 30 keV, with a

beamsize of 150 × 80 microns (h × v) at the sample position. I07 operates two end stations, an ultra-high vacuum diffractometer used for surface crystallography and a multipurpose diffractometer that is used for surface scattering, diffraction, and reflectivity experiments on polymers and soft matter systems. A double-crystal deflector can be operated along the diffractometer for supporting experiments from liquid surfaces [34]. The beamline provides a variety of sample environments (e.g. environmental cells, Langmuir troughs), as well as accommodating custom user sample environments. Multiple detectors can be used simultaneously for supporting multiscale operando and in-situ experiments combining different scattering methods (GISAXS, GIXD, XRR).

I16, a material and magnetism beamline [52], has had an active soft condensed matter community since the start of operation in 2007. I16 operates between 2.6 and 15 keV in a focal spot approximately 180 × 20 microns (h × v). Three smaller beam size options are available, two using additional KB mirrors. The first, requiring removal of the main mirrors, is used when the beam needs to be reduced to its coherent fraction with the definition of a virtual source providing a beam size of ~ 1.5 × 1.25 micron (h × v). The second mode, often requested even during coherent experiments, combines a small defocusing of the main mirrors with the use of the KB mirrors, giving a focal spot of ~ 6 × 2 micron (h × v), which contains the whole 10<sup>13</sup> photons/s provided by the source. A final combination offers a small horizontal spot with the naturally low divergent vertical focus. Beryllium-based compound refractive lenses (CRL) and Fresnel's Zone Plates (FZP) from the Diamond Optics Group have been used with measured beamsizes down to 220 nm with the FZP. Defocusing the beam to achieve beam sizes of about 300 × 300 microns (h × v) microns is possible and sometimes needed to achieve a better match with the sample dimensions and the diffractometer. The beamline allows full control of the incident photon polarization via a double phase plate retarder above 3.4 keV. The large beamline diffractometer provides support for a variety of ancillary equipment, and allows many scattering modes,

including GISAXS, GIWAXS, and XRR in non-resonant and resonant conditions. Numerous detectors are available, including in-vacuum pixelated photon counting detectors and large area photon counting detectors that can be installed at various distances to optimize the experimental strategy.

I22, Diamond's multipurpose undulator SAXS/WAXS instrument [53], has been in operation since mid-2007. The insertion device delivers X-rays with energies between 7 and 22 keV to the sample in a beamsize  $240 \times 60$  microns ( $h \times v$ ) for the main beamline, and approximately  $10 \times 10$  microns for microfocusing. The versatile sample platform can accommodate a wide range of facility and user sample environments, allowing in-operando experiments to be carried out. The beamline has had an active soft matter and polymer research program from the start, as well as activities in biological materials and environmental science.

DL-SAXS, an offline instrument purchased from Xenocs (Grenoble, France) with EPSRC funding (EP/R042683/1), maintains a steady, rapid access program for soft matter scientists working in fields as diverse as I22. The instrument comprises a dual energy X-ray source, an Excillum (Kista, Sweden) gallium metal jet delivering 9.2 keV, and a Xenocs Genix<sup>3D</sup> molybdenum microsource delivering 17.4 keV photons with approximately 200 micron beam. The in-vacuum sample chamber and detector flight tube afford excellent low background SAXS data. The sample chamber can hold many of the smaller standard I22 sample environments as well as simple solid, liquid, and gel sample holders for standard measurements.

### **Future perspectives, including Diamond II upgrade**

Diamond II will bring new opportunities to the soft matter and polymer communities. The new ring, based on double triple bend achromats (DTBAs), will bring a transformative increase in brightness and coherence and provide mid-section straights to retain and enhance all beamlines on bending magnets, while offering additional sources for five potential new beamlines. The design increases the electron beam energy from 3.0 to 3.5 GeV, providing greatly increased photon flux at higher energies for new opportunities in in-operando science. Further development of facilities at Diamond, including improved optics and X-ray detection together with continued software development for real-time data evaluation and structural modelling, will allow us to extend the range of these scales significantly and for yet smaller samples, enabling one to look much more closely at real processing conditions; for example, molecular correlations and assembly in microfluidics reactors.

This will have a very significant impact in the development of better materials for the generation, transport, and storage of energy. Organic photovoltaics, for example, are destined to play an important role in reducing our reliance on fossil fuels, in turn helping to resolve the energy crisis. Fundamental to their application is increased performance, which will only be achieved by better understanding of their morphology over multiple length scales, both in the finished device and during processing. Success could lead to materials that could coat the outside

of buildings, potentially resulting in some skyscrapers being net contributors to the national grid.

The use of molecular materials with electronic, magnetic, or optical properties may lead to new materials for the digital economy, and again, a better understanding of how their functionality depends on processing conditions through the structure they can be programmed chemically to adopt will be essential to their performance.

An improved understanding of how molecules arrange themselves in environmental media (e.g., atmospheric aerosols and colloids found in the aqueous environment) and how these arrangements impact their environmental processing would be possible with the improvements in the facilities at Diamond and the in-operando flexibility offered by beamlines such as I22.

Conscious of the plastic waste problem, the success of bio-derived and degradable alternatives to persistent plastics will rely on realizing competitive material performances. Understanding and designing in properties such as strain-induced crystallization on stretching a polymer and propensity for various phase morphologies in block copolymers will be essential. In-operando/in-situ SAXS and WAXS measurements during bulk mechanical testing will provide insight into how such behavior develops and recovers, with implications for polymer pre-processing and the realistic number of mechanical reprocessing cycles before material deterioration.

Improved understanding of the structure and disorder of polymeric and gel-based materials will be essential for their wider exploitation in healthcare; for materials to replace, repair, or accelerate the healing of biological tissue; and to develop new biosensors. Here, biomechanical and self-healing materials will play an increasing role in hospital trauma recovery where, introduced as a patch, they will integrate with the natural tissue and provide a scaffold for future skin/muscle growth. Crucial to their application will be a detailed understanding of the self-assembly and reassembly processes on the molecular level.

The Diamond-II upgrade programme will not only provide the end-stations with a brighter, and 20 times smaller (primarily in the horizontal direction), X-ray beam, it will also increase the coherent fraction of the beam by roughly a factor of 10 for photon energies larger than 1 keV targeting the application of coherent X-ray scattering techniques [4]. X-ray photon correlation spectroscopy (XPCS) at I22, for example, is currently suffering from the lack of coherent photon flux, hindering the investigation of equilibrium and out-of-equilibrium dynamics relevant in various systems (e.g., soft- and bio-materials). In combination with fast state-of-the-art detector upgrades, the technical limitations, especially for XPCS, will be exceeded and a much wider range of systems can be studied complementary to common static time-resolved X-ray scattering methods [54].

Outside of the Diamond-II upgrade programme, another area that shows great promise is that of the utilization of artificial intelligence algorithms, underpinned by machine learning, either in assisting user data analysis or, more tantalizingly, in driving experiments and measurements taking place live on the beamline. This area is increasingly becoming rich with a diverse set of use-cases being actively developed

from adaptive scanning [55], through autonomous formulation [56], and on to structural determination [57]. At Diamond, and specifically for I22, progress in this area has been made in collaboration with the on-campus Scientific Machine Learning (SciML) group which, initially, has culminated in the development of the *ffsas* software package [58] for fast colloidal systems analysis. As we move to adopting the NSLS-II-led *bluesky* scanning framework [59], we look forward to being able to adopt solutions from a wider base of sources, including collaborative efforts such as the Community for Autonomous Scientific Experimentation (CASE) [60] enabling true “intelligent” experimentation during beamtime. In addition to these exciting advances on the horizon, there are also exciting advances in molecular dynamics-driven SAS data analysis for the soft condensed matter community with packages such as Shapspyer [61], which are aimed at dramatically reducing the activation barrier for setting up complex systems to simulate “real world” systems. ■

## ORCID

- N. J. Terrill  <http://orcid.org/0000-0002-8783-1282>  
 A. Bombardi  <http://orcid.org/0000-0001-7383-1436>  
 F. Carlà  <http://orcid.org/0000-0001-8414-9934>  
 G. Cinque  <http://orcid.org/0000-0001-6801-8010>  
 M. J. Derry  <http://orcid.org/0000-0001-5010-6725>  
 A. Milsom  <http://orcid.org/0000-0003-3875-9015>  
 G. Siligardi  <http://orcid.org/0000-0002-4667-6423>  
 T. Snow  <http://orcid.org/0000-0001-7146-6885>  
 P. D. Topham  <http://orcid.org/0000-0003-4152-6976>  
 X. B. Zeng  <http://orcid.org/0000-0003-4896-8080>  
 T. Zinn  <http://orcid.org/0000-0001-8502-544X>

## References

- N. J. Brooks et al., *Chem. Phys. Lipids*. **164** (2), 89 (2011). doi:10.1016/j.chemphyslip.2010.12.002.
- N. J. Brooks et al., *Rev. Sci. Instrum.* **81** (6), 064103 (2010). doi:10.1063/1.3449332.
- B. Glettner et al., *Angew. Chem. Int. Ed.* **47** (32), 6080 (2008). doi:10.1002/anie.200802021.
- R. P. Walker, Diamond-II Technical Design Report, 2022.
- G. L. Gregory et al., *Chem. Sci.* **11** (25), 6567 (2020). doi:10.1039/d0sc00463d.
- G. L. Gregory et al., *Angew. Chem.* **61** (47), e202210748 (2022). doi:10.1002/anie.202210748.
- G. L. Gregory, and C. K. Williams, *Macromolecules*. **55** (6), 2290 (2022). doi:10.1021/acs.macromol.2c00068.
- G. L. Gregory et al., *J. Am. Chem. Soc.* **144** (38), 17477 (2022). doi:10.1021/jacs.2c06138.
- Y. X. Li et al., *Nat. Commun.* **13** (1), 384 (2022). doi:10.1038/s41467-022-28024-1.
- S. Poppe et al., *J. Am. Chem. Soc.* **142** (7), 3296 (2020). doi:10.1021/jacs.9b11073.
- C. Dressel et al., *Adv. Funct. Mater.* **30** (45), 2004353 (2020). doi:10.1002/adfm.202004353.
- R.-B. Zhang et al., *Adv. Funct. Mater.* **29** (3), 1806078 (2019). doi:10.1002/adfm.201806078.
- A. Lehmann et al., *Adv. Funct. Mater.* **28** (46), 1804162 (2018). doi:10.1002/adfm.201804162.
- X. Zeng et al., *Angew. Chem. Int. Ed.* **55** (29), 8324 (2016). doi:10.1002/anie.201602734.
- S. Poppe et al., *Nat. Commun.* **6** (1), 8637 (2015). doi:10.1038/ncomms9637.
- R. Zhang et al., *ACS Nano*. **8** (5), 4500 (2014). doi:10.1021/nn406368e.
- F. Liu et al., *Nat. Commun.* **3** (1), 1104 (2012). doi:10.1038/ncomms2096.
- X. Zeng et al., *Science*. **331** (6022), 1302 (2011). doi:10.1126/science.1193052.
- M. Prehm et al., *J. Am. Chem. Soc.* **133** (13), 4906 (2011). doi:10.1021/ja110065r.
- W. D. Stevenson et al., *Phys. Chem. Chem. Phys.* **19** (21), 13449 (2017). doi:10.1039/c7cp01404j.
- D. T. W. Toolan et al., *Phys. Chem. Chem. Phys.* **19** (31), 20412 (2017). doi:10.1039/c7cp03578k.
- W. Bras et al., *Science*. **267** (5200), 996 (1995). doi:10.1126/science.267.5200.996.
- E. E. Brotherton et al., *J. Am. Chem. Soc.* **141** (34), 13664 (2019). doi:10.1021/jacs.9b06788.
- D. J. Keddie, *Chem. Soc. Rev.* **43** (2), 496 (2014). doi:10.1039/c3cs60290g.
- R. L. Atkinson et al., *Eur. Polym. J.* **179**, 111567 (2022). doi:10.1016/j.eurpolymj.2022.111567.
- R. L. Atkinson et al., *Polym. Chem.* **12** (21), 3177 (2021). doi:10.1039/d1py00326g.
- M. J. Derry et al., *Chem. Sci.* **7** (8), 5078 (2016). doi:10.1039/c6sc01243d.
- S. D. P. Fielden et al., *J. Am. Chem. Soc.* **145** (10), 5824 (2023). doi:10.1021/jacs.2c13049.
- A. Milsom et al., *Atmos. Chem. Phys.* **21** (19), 15003 (2021). doi:10.5194/acp-21-15003-2021.
- A. Milsom et al., *Faraday Discuss.* **226**, 364 (2021). doi:10.1039/d0fd00088d.
- A. Milsom et al., *Atmos. Chem. Phys.* **22** (7), 4895 (2022). doi:10.5194/acp-2021-919. 10.5194/acp-22-4895-2022
- P. N. Jemmett et al., *Langmuir*. **38** (46), 14290 (2022). doi:10.1021/acs.langmuir.2c02370.
- A. L. Martin et al., *Langmuir*. **39** (7), 2676 (2023). doi:10.1021/acs.langmuir.2c03161.
- T. Arnold et al., *J. Synchrotron Rad.* **19** (3), 408 (2012). doi:10.1107/S0909049512009272.
- C. Nicklin et al., *Rev. Sci. Instrum.* **88** (10), 103901 (2017). doi:10.1063/1.4989761.
- S. J. T. Brugman et al., *J. Phys. Chem. C*. **126** (20), 8855 (2022). doi:10.1021/acs.jpcc.2c01157.
- R. Hussain et al., *Front. Chem.* **9**, 616928 (2021). doi:10.3389/fchem.2021.616928.
- G. Albano et al., *Aggregate*. **3** (5), e193 (2022). doi:10.1002/agt2.193.
- S. R. Clowes et al., *Molecules*. **28** (4), 1523 (2023). doi:10.3390/molecules28041523.
- C. E. Killalea et al., *Chem. Commun.* **58** (28), 4468 (2022). doi:10.1039/d1cc06790g.
- J. M. Martin, and A. Erdemir, *Phys. Today*. **71** (4), 40 (2018). doi:10.1063/pt.3.3897.
- T. Reddyhoff et al., *ACS Appl. Mater. Interfaces*. **13** (7), 9239 (2021). doi:10.1021/acsami.0c21918.
- F. Walton et al., *J. Am. Chem. Soc.* **142** (16), 7591 (2020). doi:10.1021/jacs.0c01712.
- G. Cinque et al., *Synchr. Radiation News*. **24** (5), 24 (2011). doi:10.1080/08940886.2011.618093.
- L. Quaroni et al., *Faraday Discuss.* **187** (0), 259 (2016). doi:10.1039/c5fd00156k.

46. M. Azizian Kalkhoran et al., *Opt. Lett.* **47** (12), 2959 (2022). doi:10.1364/OL.456049.
47. A. F. Möslein et al., *Adv. Materials Inter.* **10** (3), 2201401 (2023). doi:10.1002/admi.202201401.
48. L. A. E. Batista de Carvalho et al., *Biophys. J.* **120** (15), 3070 (2021). doi:10.1016/j.bpj.2021.06.012.
49. P. M. Donaldson et al., *Opt. Express.* **24** (3), 1852 (2016). doi:10.1364/OE.24.001852.
50. T. Javorfi et al., *Chirality.* **22** (1E), E149 (2010). doi:10.1002/chir.20924.
51. C. Nicklin et al., *J. Synchrotron Rad.* **23** (5), 1245 (2016). doi:10.1107/S1600577516009875.
52. S. P. Collins et al., *AIP Conf. Proc.* **1234** (1), 303 (2010). doi:10.1063/1.3463196.
53. A. J. Smith et al., *J. Synchrotron Rad.* **28** (3), 939 (2021). doi:10.1107/S1600577521002113.
54. T. Narayanan et al., *J. Appl. Crystallogr.* **55** (1), 98 (2022). doi:10.1107/S1600576721012693.
55. M. M. Noack et al., *Sci. Rep.* **9** (1), 11809 (2019). doi:10.1038/s41598-019-48114-3.
56. P. A. Beaucage, and T. B. Martin, *Chem. Mater.* **35** (3), 846 (2023). doi:10.1021/acs.chemmater.2c03118.
57. M. Baek et al., *Science.* **373** (6557), 871 (2021). doi:10.1126/science.abj8754.
58. K. Leng et al., *J. Appl. Crystallogr.* **55** (4), 966 (2022). doi:10.1107/S1600576722006379.
59. D. Allan et al., *Synch. Radiation News.* **32** (3), 19 (2019). doi:10.1080/08940886.2019.1608121.
60. M. Noack, and J. Sethian, Autonomous discovery in science and engineering. Technical Report, 2021. doi:10.2172/1818491.
61. A. Brukhno, *Shapespyer: Python-driven Toolchain for Modelling Soft Matter*, 2022. <https://www.scd.stfc.ac.uk/Pages/Shapespyer.aspx>.